A Case Study of 5G gNodeB Throughput Analysis Using Practical KPIs

Rômulo Torres Serra and Maurício Henrique Costa Dias

***Abstract*—Enhanced mobile broadband is one of the three major operating scenarios of 5G, directly impacting the average mobile user. Therefore, capacity planning is crucial for providing excellent user experience. The 3GPP, in its TS 38.306 specification, established a theoretical model to estimate maximum throughput values. However, this equation presents challenges for real usage analysis because capacity is tracked in practice using key performance indicators (KPIs) that do not entirely correspond to the model's input parameters. This paper presents a case study of real 5G gNodeB throughput, integrating practical KPIs within the 3GPP model framework. Various tests were conducted in different usage scenarios, comparing real measured throughput with predictions using a proposed hybrid version of the 3GPP model. A good correlation between predictions and measurements was observed regarding hourly throughput variation. Additionally, it was found that considering the actual use of the available bandwidth, rather than assuming all resource blocks are fully occupied at all times, applying a scale factor can improve the predictions, leading to a good convergence with the measurements.**

***Index Terms*—3GPP, 5G, capacity, link budget, throughput.**

I. INTRODUCTION

NETWORK Planning is a multifaceted task that encompasses several critical aspects. Within this framework, calculating the link budget with accurate data and a variety of parameters is essential for optimal sizing. At this stage, a theoretical study is conducted, which enables the final power calculation throughout the entire path from transmission to reception. This process takes into account transmission power, various equipment losses, antenna and amplifiers gains, and propagation effects. Separate calculations are performed for downlink and uplink due to the differing parameters in each transmission direction.

In this context, the capacity study emerges as one of the key aspects to be considered in mobile network planning and engineering. 5G development is guided by three main operating scenarios: ultra-reliable low latency communications (URLLC), massive machine-type communication (mMTC), and enhanced mobile broadband (eMBB). The eMBB scenario specifically addresses the high data transmission rates and large traffic volumes demanded by 5G New Radio (5G NR), necessitating detailed capacity planning to ensure a high-quality user experience.

3GPP recommends the using a theoretical maximum throughput equation in TS 38.306 [1] as a basis for capacity studies in 5G radio access network planning. While this equation is intended to be helpful at the early planning stages, it presents a few issues when used for real usage analyses or predictions based on actual usage. Some of the equation parameters are not tracked directly by the cell or site. Instead, throughput performance is measured using a few Key Performance Indicators (KPIs) that are straightforwardly present in the equation.

One of the primary KPIs tracked in practice is the Channel Quality Indicator (CQI), which is not directly included in the 3GPP TS 38.306 equation. However, according to 3GPP TS 36.213 [2], there is a direct correlation between CQI and the product of two equation parameters corresponding to spectral efficiency [3]. Furthermore, the original equation includes the number of resource blocks allocation, mainly in the context of maximum usage. In practice, however, resource blocks allocation is dynamic. Therefore, for real usage analysis, instead of a fixed maximum value, a real KPI tracking this allocation over time should be considered.

The objective of this paper is to analyze a few cases of real throughput data within the framework of the 3GPP theoretical model, incorporating practical KPIs. To achieve this, a case study was conducted, measuring the throughput of a few gNodeB stations in Rio de Janeiro during the months of April and May 2024. The analysis focused on typical, regular traffic, as well as traffic from atypical events. Hybrid predictions, using the theoretical model informed by real data from specific KPIs, were derived and compared to the measured throughputs.

This paper is organized as follows. Section II addresses the necessary fundamentals of this work. Section III explains the conception and execution of the case study. Section IV presents the analysis, comparing capacity predictions with real throughput data and discussing the results obtained. Finally,

Rômulo T. Serra, TIM BRASIL, RJ, Brazil.
(e-mail: rtserra@timbrasil.com.br; ORCID: 0000-0001-7326-761X)
Maurício H. C. Dias, Centro Federal de Educação Tecnológica Celso Suckow da Fonseca (CEFET/RJ), RJ, Brazil.
(e-mail: mauricio.dias@cefet-rj.br; ORCID: 0000-0002-5545-251X)
Submission: 2024-08-25, First decision: 2024-12-11, Acceptance: 2025-04-10, Publication: 2025-04-29.
Digital Object Identifier: 10.14209/jcis.2025.11

Section V provides concluding remarks.

II. FUNDAMENTALS

A. 3GPP Maximum Throughput Equation

For calculating the approximate throughput value in 5G for a given number of aggregated carriers in a band or band combination [1], the following equation is used:

$$C = 10^{-6} \cdot \sum_{j=1}^{J} \{ V_{layers}^{(j)} \cdot Q_m^{(j)} \cdot f^{(j)} \cdot R_{max} \cdot \frac{N_{PRB}^{BW(j),\mu} \cdot 12}{T_S^{\mu}} \cdot (1 - OH^{(j)}) \}. \quad (1)$$

In (1), the parameters are described as follows: C corresponds to the theoretical maximum throughput value, in Mbps. J is the number of component carriers aggregated in a band or a combination of bands (according to 3GPP TR 38.802 [4], the maximum number of NR carriers is 16). $V_{layers}^{(j)}$ is the maximum number of layers for each carrier (the maximum value is 4 for uplink and 8 for downlink). It is worth noting that layers represent the number of transmission flows from the gNodeB to the user equipment (UE) in downlink, and vice-versa in uplink [5]. $Q_m^{(j)}$ is the maximum modulation order: 2 for QPSK, 4 for 16-QAM, 6 for 64-QAM, and 8 for 256-QAM. $f^{(j)}$ is the scaling factor, which can take values of 1, 0.8, 0.75, or 0.4. R_{max} is the maximum coding rate, with a value of 0.92578125. μ is numerology, a key parameter that affects the bandwidth and performance of a 5G network. 5G supports various subcarrier spacing (SCS) values, including 15 kHz, 30 kHz, 60 kHz, 120 kHz, and 240 kHz. These SCS values are mapped to numerologies 0, 1, 2, 3, and 4, respectively. The higher the numerology, the wider the SCS [6]. $N_{PRB}^{BW(j),\mu}$ is the maximum allocation of physical resource blocks (PRBs) in a bandwidth $BW(j)$ for a given numerology μ. $BW(j)$ is the supported maximum bandwidth in each band or in band combinations. T_S^{μ} is the average duration of an OFDM symbol in a subframe, given the value of μ for a normal cyclic prefix, calculated as $10^{-3}/(14 \cdot 2^{\mu})$. Finally, $OH^{(j)}$ is the overhead, which can take values of 0.14 in downlink and 0.08 in uplink for the frequency range from 450 MHz to 6000 MHz and 0.18 in downlink and 0.10 in uplink for the frequency range from 24250 MHz to 52600 MHz. The product of the parameters $Q_m^{(j)}$ and R_{max} provides spectral efficiency (SE), which is correlated with CQI, as discussed next.

B. Practical 5G Key Performance Indicators

There are several KPIs that phone carriers use to monitor their network performance and observe daily usage behavior, such as mean user throughput, mean number of active users, CQI, mean PRBs used, and more. This data is collected by a gNodeB from field measurements and processed to provide visualizations for monitoring purposes. Mean values are calculated within regular intervals, with one-hour windows being a typical choice, as considered in this work. These KPIs serve as the reference for analyzing network quality and consequently for network planning and strategic decision-making regarding coverage expansion and capacity reinforcement.

All these KPIs can be analyzed for downlink and uplink scenarios. It is important to note that CQI assumes values in the range from 0 (worst quality) to 15 (best quality), and it is used by the system to dynamically adapt the modulation order and code rate during a link operation [7].

C. Relation of CQI to Spectral Efficiency

CQI is control information used within a mobile network to determine the utilization of the available spectral resources by the user equipment. Based on this information, the gNodeB adjusts the resource dispatch conditions, the modulation scheme selection, and the coding rate to be applied to the resource blocks requested by the user. Therefore, as CQI increases, spectral efficiency also increases, resulting in throughput optimization [8].

The 3GPP TS 36.213 specification [2] addresses the correlation between CQI and the possible modulation orders combined with the code rate values, which provide the spectral efficiency range when multiplied. This correlation is presented in tabular form, associating SE only with integer values of CQI, as shown in Table I. Consequently, this table was a natural asset to consider in the analysis conducted in this work, as CQI was chosen as a KPI to be properly incorporated into (1).

After close inspection of Table I, it can be observed that there is an almost linear relationship between SE and CQI. Thus, to facilitate the use of CQI as an input for the intended adaptation of (1), linear and quadratic regression fits were performed, as given by (2) and (3), respectively. Fig. 1 shows the relationship between SE and CQI, using data from Table I and overlaying both fit curves. The convergence is clear. Both the linear and quadratic regression fits presented the same mean error ($1.75 \cdot 10^{-5}$), but the quadratic regression exhibited a lower mean square error ($5.307 \cdot 10^{-3}$ versus $23.028 \cdot 10^{-3}$ for the linear regression fit). Since the linear fit provides negative SE values for CQI < 1.3 and the quadratic regression fit was superior, the latter was chosen for the remainder of this work.

$$\mathrm{SE} = 0.5288 \cdot \mathrm{CQI} - 0.704 \quad (2)$$

$$\mathrm{SE} = 8.027 \cdot 10^{-3} \cdot \mathrm{CQI}^2 + 0.4 \cdot \mathrm{CQI} - 0.34 \quad (3)$$

D. Hybrid Equation

A hybrid equation for C was proposed keeping most of the original parameters from (1) but replacing $Q_m^{(j)}$ and R_{max} by SE and adapting $N_{PRB}^{BW(j),\mu}$ as follows:

$$C = 10^{-6} \cdot \sum_{j=1}^{J} \{ V_{layers}^{(j)} \cdot \mathrm{SE} \cdot f^{(j)} \cdot \cdot \frac{\mathrm{PRB_{USED\ MEAN}} \cdot 12}{T_S^{\mu}} \cdot (1 - OH^{(j)}) \}. \quad (4)$$

In (4), $PRB_{USED\ MEAN}$ replaces $N_{PRB}^{BW(j),\mu}$ since it represents the collected KPI that provides the mean utilization of resource blocks for the available bandwidth within a one-hour period.

TABLE I
3GPP TS 36.213 CQI TABLE – 256QAM (ADAPTED FROM [2]).

CQI index	modulation	code rate × 1024	efficiency
0	out of range		
1	QPSK	78	0.1523
2	QPSK	193	0.3770
3	QPSK	449	0.8770
4	16QAM	378	1.4766
5	16QAM	490	1.9141
6	16QAM	616	2.4063
7	64QAM	466	2.7305
8	64QAM	567	3.3223
9	64QAM	666	3.9023
10	64QAM	772	4.5234
11	64QAM	873	5.1152
12	256QAM	711	5.5547
13	256QAM	797	6.2266
14	256QAM	885	6.9141
15	256QAM	948	7.4063

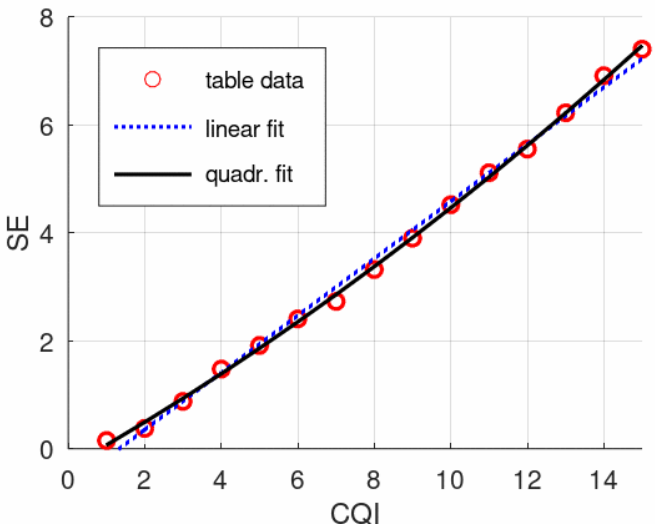

Fig. 1. SE versus CQI as provided in [3]: table data and fits.

III. METHODOLOGY

To enhance understanding, both downlink and uplink scenarios were considered in this study, utilizing real measurements from gNodeBs located at strategic points throughout Rio de Janeiro. The first gNodeB is situated on Atlantic Avenue at Copacabana Beach, with measurements conducted during the week spanning from May 1st to May 8th, 2024. This specific venue and week were chosen because they allowed the observation of regular traffic on most days, as well as atypical throughput demanded by a huge music concert on May 4th, 2024. This approach enabled a comparative analysis between typical behavior and high network congestion for the same site.

The second gNodeB is located on Abelardo Bueno Avenue, in Barra da Tijuca. This venue was chosen because it allows observation of typical traffic behavior, as well as intense vehicle traffic during peak hours. Additionally, this avenue hosts arenas where seasonal events occur. Notably, on May 8th, 2024, there was an event available that suited this case study.

The third gNodeB is located on the Sugar Loaf cable car, one of the most iconic tourist attractions in Rio de Janeiro. The site features a small cell at the cable car boarding station. This location was chosen due to the high daily tourist traffic. In addition, a music festival took place on the weekends between April 5th and 27th, 2024, which resulted in atypical traffic, especially at night. This scenario differs from the previous ones because it involves a 5G site operating in the 2300 MHz frequency band using Dynamic Spectrum Sharing (DSS). This point is significant for observing performance with a different configuration scenario.

DSS is a resource for the initial stage of 5G network deployments and is advantageous for an expanding market, as it allocates time and frequency resources proportional to user traffic demand, providing better spectrum utilization. The technology is designed to be backward compatible with existing LTE UEs. Since 4G and 5G are likely to coexist for an extended period, the adoption of spectrum sharing facilitates the transition period between generations. However, DSS introduces challenges, such as reduced network capacity and peak throughput achievable by individual users due to the overhead generated from NR and LTE control channels. The actual reduction in capacity varies depending on the DSS implementation and configuration. The role of DSS is to allow the allocation of NR users to the LTE spectrum without affecting the essentials of one system for the other [9].

The following KPIs were collected daily and averaged hourly: mean user throughput, mean number of active users, CQI, and mean PRBs used. It is crucial to understand some gNodeB parameters that directly influence the case study proposal analysis. Tables II, III and IV present the configuration details of the Copacabana, Barra da Tijuca and Sugar Loaf gNodeBs, respectively.

Overall, the primary goal was to conduct a comparative analysis between the mean throughput values measured hourly over one or more days from the selected gNodeBs and the corresponding hybrid theoretical predictions as derived by (4). It was anticipated that some form of correlation or convergence would emerge.

TABLE II
CONFIGURATION PARAMETERS USED IN COPACABANA GNODEB.

Configuration Parameter Name	Parameter Value
5G StandAlone	Yes
Operational Frequency	3500 MHz
Available Bandwidth	100 MHz
Sub-Carrier Spacing	30 kHz
MIMO Configuration	64T64R
Layers	2 UL / 6 DL

TABLE III
CONFIGURATION PARAMETERS USED IN BARRA DA TIJUCA GNODEB.

Configuration Parameter Name	Parameter Value
5G StandAlone	Yes
Operational Frequency	3500 MHz
Available Bandwidth	100 MHz
Sub-Carrier Spacing	30 kHz
MIMO Configuration	64T64R
Layers	2 UL / 6 DL

TABLE IV
CONFIGURATION PARAMETERS USED IN SUGAR LOAF GNODEB.

Configuration Parameter Name	Parameter Value
5G StandAlone	No (DSS)
Operational Frequency	2300 MHz
Available Bandwidth	40 MHz
Sub-Carrier Spacing	30 kHz
MIMO Configuration	2T2R
Layers	2 UL / 2 DL

Some fixed parameters of the gNodeBs used in (4) were: J, the number of carriers (in this work it is only 1); $V_{layers}^{(j)}$, the number of layers, configured according to the equipment (in this work it was 2 for uplink and 6 for downlink); $f^{(j)}$, the scaling factor, which in the current baseline is equal to 1; T_s^{μ}, the average duration of an OFDM symbol in a subframe (35.714 µs here); and finally $OH^{(j)}$, which was 0.14 for downlink and 0.08 for uplink, in the operating frequency bands.

SE and $PRB_{USED\ MEAN}$ were provided from the hourly KPIs collected from the gNodeBs. For each one-hour window, the hybrid theoretical throughput, calculated by (4), was then compared to the corresponding measured throughput of the site. The measured throughput was given by the mean user throughput multiplied by the mean number of active users.

IV. CASE STUDY

A. Overall Regular Traffic

Fig. 2, Fig. 3 and Fig. 4 present a comparison between the theoretical downlink throughput calculated using the hybrid prediction model with practical KPIs and the downlink throughput measurements of the Copacabana Beach gNodeB (May 3rd), the Barra da Tijuca gNodeB (May 6th), and the Sugar Loaf gNodeB (April 25th) in 2024, respectively. In these figures, the vertical axis on the left represents the theoretical throughput, while the vertical axis on the right represents the measured throughput. These measurements were taken on business days when typical traffic patterns were observed at these sites. Furthermore, as Fig.4 pertains to a 5G DSS site, it supports the view of [9], indicating a reduction in network capacity and the peak throughput achievable by individual users due to the overload generated from NR and LTE control channels.

A clear correlation is observed between the behaviors of real measurements and the adjusted equation's theoretical results. However, there is a considerable difference between the magnitude scales of the throughput values. Good convergence is achieved only when the theoretical throughput is multiplied by a *scale* factor (SF), which functions as a measure of discrepancy between theoretical and actual measurements. It roughly corresponds to the measured throughput axis range (MTAR) divided by the theoretical throughput axis range (TTAR), as shown in (5). It is worth noting that this *scale* factor is unrelated to the *scaling* factor $f^{(j)}$ in (1). Fig. 5, Fig. 6 and Fig. 7 illustrate the outcome of this adjustment to the curves plotted in Fig. 2, Fig. 3 and Fig. 4, respectively.

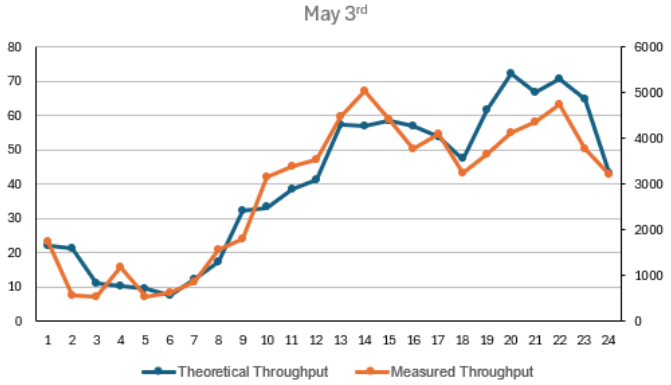

Fig. 2. Hourly variation of theoretical and measured throughput (Mbps) of Copacabana gNodeB for downlink on May 3rd.

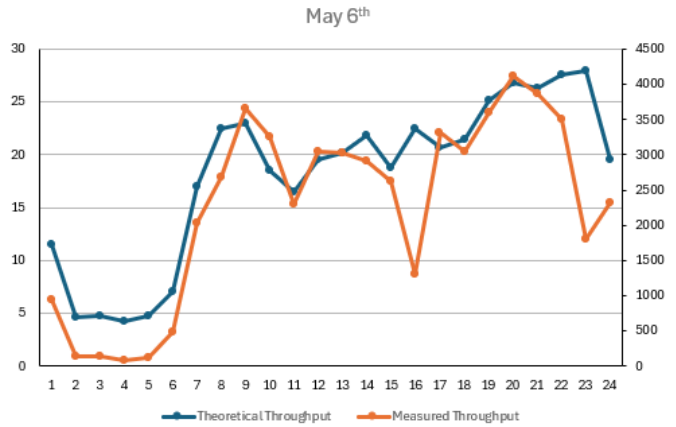

Fig. 3. Hourly variation of theoretical and measured throughput (Mbps) of Barra da Tijuca gNodeB for downlink on May 6th.

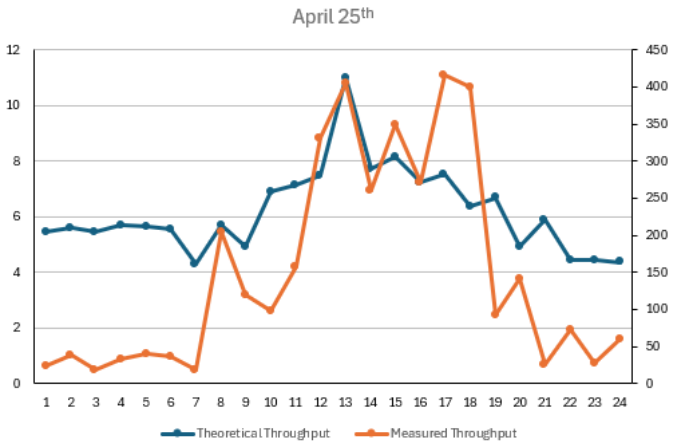

Fig. 4. Hourly variation of theoretical and measured throughput (Mbps) of Sugar Loaf gNodeB for downlink on April 25th.

$$SF = MTAR / TTAR \quad (5)$$

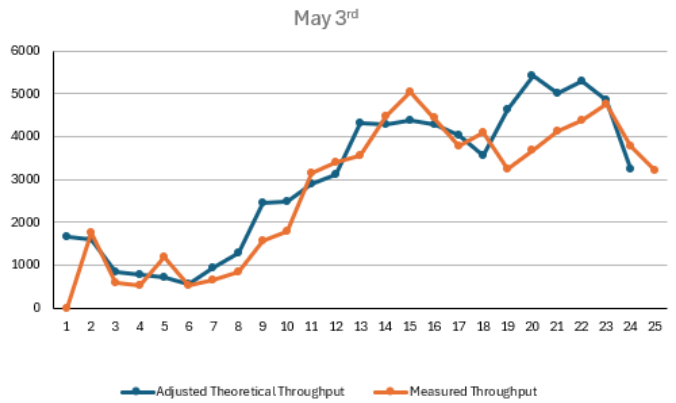

Fig. 5. Hourly variation of theoretical throughput (Mbps) adjusted with a single SF = 75, and measured throughput (Mbps) of Copacabana gNodeB for downlink on May 3rd.

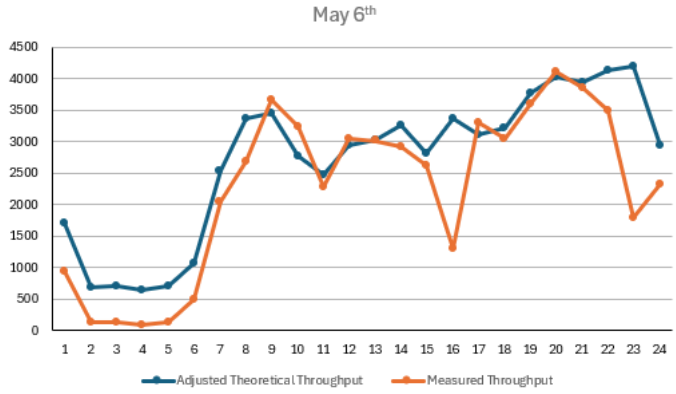

Fig. 6. Hourly variation of theoretical throughput (Mbps) adjusted with a single SF = 150, and measured throughput (Mbps) of Barra da Tijuca gNodeB for downlink on May 6th.

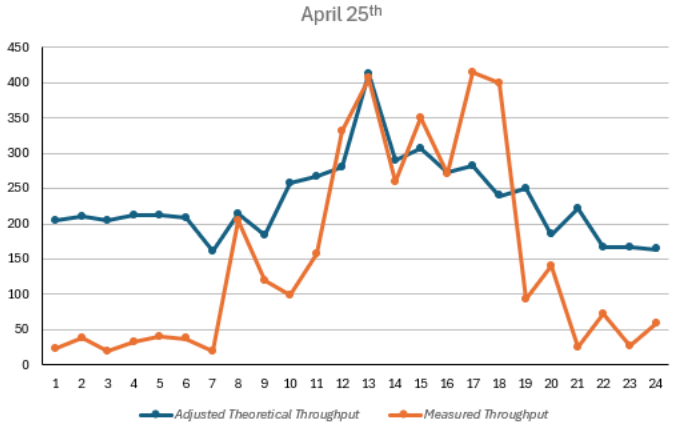

Fig. 7. Hourly variation of theoretical throughput (Mbps) adjusted with a single SF = 37.5, and measured throughput (Mbps) of Sugar Loaf gNodeB for downlink on April 25th.

A natural discussion arises from the large SF values, despite the clear correlation between the daily behaviors of theoretical and real throughput. A possible explanation is that the typical cell phone usage by users today, on regular traffic days, does not result in PRB allocation that fully exploits the entire bandwidth potential. Consequently, the hourly average $PRB_{USED\ MEAN}$ KPI derived from measurements, if used as is in (1), leads to an underestimated throughput prediction. Therefore, ideally, to use this KPI without the need for a correction scale factor, the allocated PRB should be fully exploited throughout the hour. Such a scenario is expected to occur under high traffic demand conditions. Considering the downlink-uplink asymmetry, such high demand instances are more likely to be observed in uplink traffic.

Fig. 8 and Fig 9 compare the hourly variation of the hybrid prediction and measurements for the uplink case of the Copacabana beach gNodeB and a busy avenue in Barra da Tijuca. Notably, there was no need for a scale factor in these cases. In Fig. 8, there is a clear correlation, with theoretical and measured throughput values in the same range. Furthermore, it is worth observing that, in Fig. 9, during peak traffic times between 6 and 8 pm, the increased network usage brings the curves closer together. This observation seemingly

corroborates the previously discussed hypothesis regarding the difference between predicted and measured throughput.

Due to a lack of consistent data in the samples collected for the uplink, the Sugar Loaf gNodeB was not considered for uplink tests. The hourly average number of connected users was very low, making comparative graphical analysis between theoretical and real throughput unfeasible.

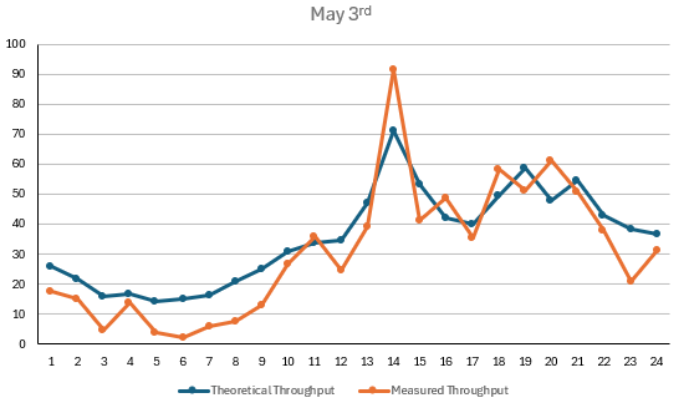

Fig. 8. Hourly variation of theoretical and measured throughput (Mbps) of Copacabana gNodeB for uplink on May 3rd.

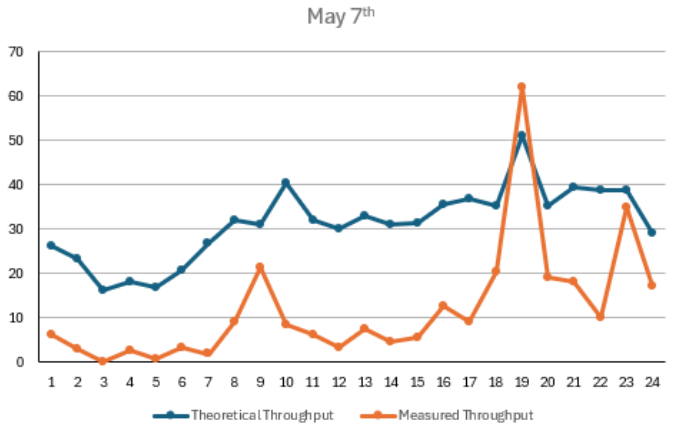

Fig. 9. Hourly variation of theoretical and measured throughput (Mbps) of Barra da Tijuca gNodeB for uplink on May 7th.

B. Traffic During Atypical Day

On May 4th, 2024, Copacabana beach hosted a major event. The estimated audience at the concert was around 1.6 million people, making it a completely atypical day compared to the usual traffic. The test results were analyzed, focusing on the hourly traffic evolution throughout the day and observing the peak at the time the show took place.

Unlike the regular traffic cases observed, the correlation between measured and theoretical throughputs was not consistent throughout the whole day but rather appeared in blocks of a few hours. To achieve compatible figures, an adjusted scale factor (SF_a) should be applied accordingly, multiplying SF in (5) by a reduction factor k, as shown in (6).

$$SF_a = k \cdot SF \quad (6)$$

Fig. 10 compares the hourly variation of the measurements and the hybrid prediction using (6). Table V presents the adjusted theoretical predictions with their respective hourly adjusted scale factors (SF_a). An initial SF of 75 was adopted as the regular reference scale factor, showing good adherence during the initial part of the day when traffic followed its usual behavior in the region. As the hours passed and the event time approached, the number of connected users significantly increased, as did the actual usage of available bandwidth for each PRB. This led to a progressive reduction of the initial scale factor, reaching its minimum between 8 and 10 pm, the time of the show, when there was the largest number of active users and a peak in traffic.

The analysis of such an atypical day provides further evidence supporting the previously stated hypothesis: a situation of higher network stress brings better convergence between theoretical predictions calculated using the hybrid equation (4) and real traffic.

TABLE V
HYBRID PREDICTED THROUGHPUT AND SCALE FACTORS OBSERVED AT COPACABANA GNODEB FOR DOWNLINK ON MAY 4TH.

Hour	Adjusted Theoretical Throughput (Mbps)	k	SF_a
12:00 AM	2239.14	1	75
01:00 AM	1596.74	1	75
02:00 AM	1729.57	1	75
03:00 AM	1169.22	1	75
04:00 AM	1110.32	1	75
05:00 AM	785.94	1	75
06:00 AM	1177.72	1	75
07:00 AM	1411.36	1	75
08:00 AM	2183.94	1	75
09:00 AM	2808.25	1	75
10:00 AM	3599.37	1	75
11:00 AM	3274.10	1.50	50
12:00 PM	3040.13	1.50	50
01:00 PM	3928.63	1.50	50
02:00 PM	4188.44	1.50	50
03:00 PM	3879.56	1.50	50
04:00 PM	3717.54	2	37.50
05:00 PM	4039.73	2	37.50
06:00 PM	2997.80	3	25
07:00 PM	2935.45	4	18.75
08:00 PM	2357.70	5	15
09:00 PM	2472.72	5	15
10:00 PM	2186.94	5	15
11:00 PM	2655.23	3	25

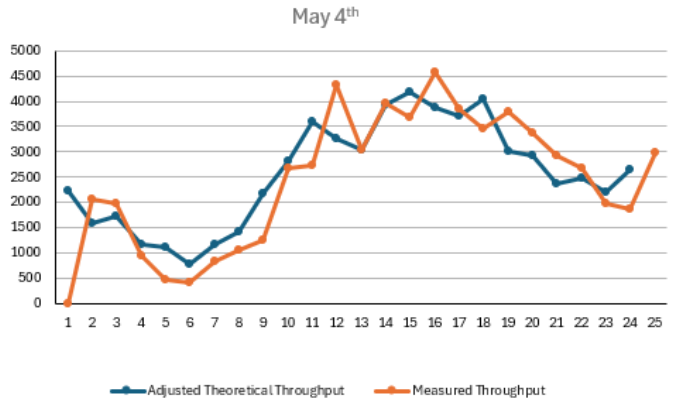

Fig. 10. Hourly variation of theoretical throughput (Mbps) adjusted with different SF per hour, and measured throughput (Mbps) of Copacabana gNodeB for downlink on May 4th.

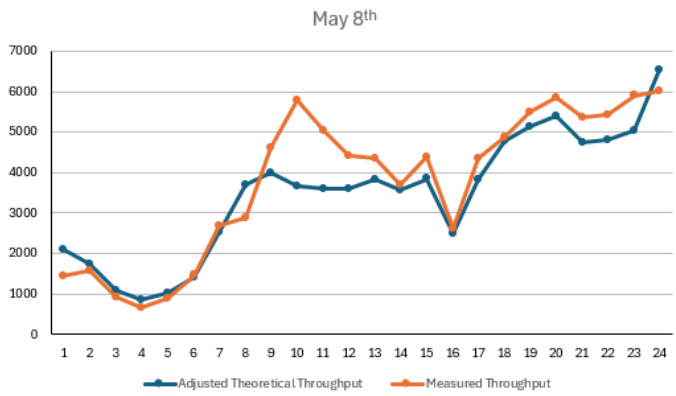

Fig. 11. Hourly variation of theoretical throughput (Mbps) adjusted with different SF per hour, and measured throughput (Mbps) of Barra da Tijuca gNodeB for downlink on May 8th.

On May 8th, 2024, a concert with a large audience took place in one of the Olympic Park arenas in Barra da Tijuca, increasing the number of connected users at night compared to the region's usual weekday traffic. Fig. 11 compares the hourly variation of measurements and hybrid forecast for the downlink, using different scale factors each hour. Table VI presents the theoretical predictions adjusted with their respective hourly adjusted scale factors and reduction factors.

An initial SF of 150 was adopted as a standard reference factor, showing good adherence in the morning. During the afternoon and evening, with peak traffic hours on the avenue combined with the large movement for the show, there was an increase in the number of connected users and consequently a reduction in the SF. On a day with slightly higher than usual traffic on that busy road, a situation of greater network stress brought better convergence between the predictions calculated by the hybrid equation and the real measurements.

On April 25th, 2024, in addition to the large number of tourists who regularly visit Sugar Loaf, there was an event with a concert at Morro da Urca that also impacted the cable car traffic at night. As seen in previous scenarios, Fig 12 compares the hourly variation of measurements and hybrid forecast for the downlink, using different scale factors each hour. Due to the unique characteristics and behavior of this scenario – where the reference gNodeB is a small cell in a closed environment with better CQI levels and utilizes 5G DSS technology – a single reference scale factor was not adopted. Instead, a different scale factor was used for each hour. Table VII presents the hybrid theoretical predictions adjusted with their respective hourly scale factors.

Fig. 13 compares the hourly variation of measurements and the hybrid prediction on the event day in Copacabana, now considering uplink. Unlike the downlink cases, the correlation between the curves can be seen within the same throughput range (300 to 350 Mbps). This is due to the type of UE usage during events like this, where photos and videos are posted in large volumes, and a high number of live streams occur, consuming substantial bandwidth in the uplink.

TABLE VI
HYBRID PREDICTED THROUGHPUT AND SCALE FACTORS OBSERVED AT BARRA DA TIJUCA GNODEB FOR DOWNLINK ON MAY 8TH.

Hour	Adjusted Theoretical Throughput (Mbps)	k	SF_a
12:00 AM	2110.60	1	150
01:00 AM	1725.76	1	150
02:00 AM	1079.59	1	150
03:00 AM	864.29	1	150
04:00 AM	1013.59	1	150
05:00 AM	1427.48	1	150
06:00 AM	2530.18	1	150
07:00 AM	3712.14	1	150
08:00 AM	4005.77	1	150
09:00 AM	3671.19	1	150
10:00 AM	3598.80	1	150
11:00 AM	3596.92	1	150
12:00 PM	3822.19	1.25	120
01:00 PM	3580.48	1.25	120
02:00 PM	3847.04	1	150
03:00 PM	2482.76	2	75
04:00 PM	3818.05	1.5	100
05:00 PM	4772.34	2	75
06:00 PM	5148.46	1.5	100
07:00 PM	5386.94	1	150
08:00 PM	4739.75	1.25	120
09:00 PM	4809.57	1.25	120
10:00 PM	5024.05	1.25	120
11:00 PM	6556.09	1	150

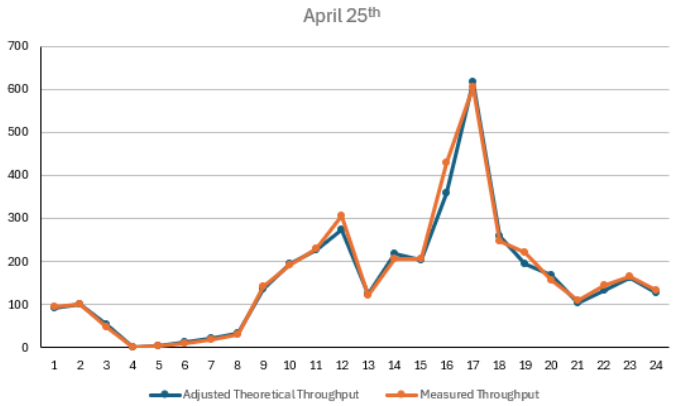

Fig. 12. Hourly variation of theoretical throughput (Mbps) adjusted with different SF per hour, and measured throughput (Mbps) of Sugar Loaf gNodeB for downlink on April 25th.

TABLE VII
HYBRID PREDICTED THROUGHPUT AND SCALE FACTORS OBSERVED AT SUGAR LOAF GNODEB FOR DOWNLINK ON APRIL 25TH.

Hour	Adjusted Theoretical Throughput (Mbps)	SF
12:00 AM	91.02	12.96
01:00 AM	100.41	14.14
02:00 AM	53.71	7.77
03:00 AM	1.11	0.19
04:00 AM	3.77	0.64
05:00 AM	11.84	2.16
06:00 AM	21.49	4.86
07:00 AM	32.82	6.48
08:00 AM	136.90	22.22
09:00 AM	193.85	31.11
10:00 AM	226.86	17.28
11:00 AM	275.43	38.89
12:00 PM	125.38	17.28
01:00 PM	217.89	31.11
02:00 PM	202.79	22.22
03:00 PM	359.20	38.89
04:00 PM	617.59	38.89
05:00 PM	260.49	31.11
06:00 PM	194.50	25.92
07:00 PM	168.68	25.92
08:00 PM	104.50	19.44
09:00 PM	132.14	19.44
10:00 PM	161.43	19.44
11:00 PM	128.00	19.44

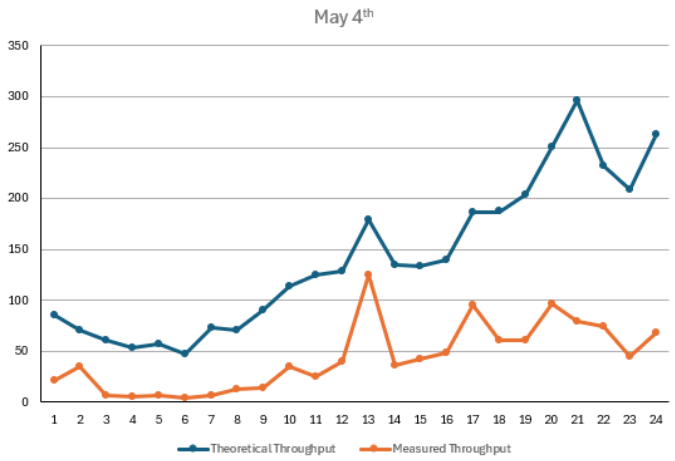

Fig. 13. Hourly variation of theoretical and measured (Mbps) throughput of Copacabana gNodeB for uplink on May 4th.

Fig. 14 compares the hourly variation of measurements and hybrid predictions on May 8th, 2024, on Abelardo Bueno Avenue, considering the uplink. On this day, a concert with a large audience took place in one of the Olympic Park's arenas, increasing the traffic at night compared to the usual weekday traffic. There is a similarity in the curves' behavior, with values on the same magnitude scale, without the need for a scaling factor. A larger difference is observed during the first hours of the day when the number of connected users is zero or very low. The curves converge during peak traffic hours and after 11 pm, when the event ended, and a large concentration of people walked through this avenue.

For the uplink, a good convergence was observed without the need for a scaling factor due to its usage characteristics. It is important to note an increase in theoretical throughput during peak traffic times, due to increased PRB utilization, which directly impacts the capacity equation.

Again, due to a lack of consistent data in the collected samples, the uplink was not considered for the atypical day analysis in the Sugar Loaf gNodeB. The hourly average number of connected users was very low, making comparative graphical analysis between theoretical and real measured throughput unfeasible.

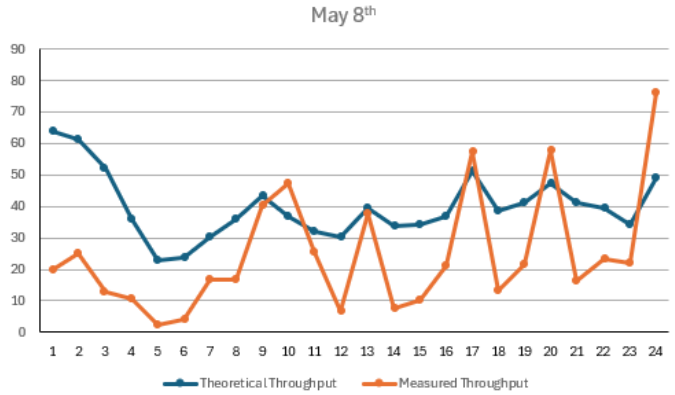

Fig. 14. Hourly variation of theoretical and measured throughput of Barra da Tijuca gNodeB for uplink on May 8th.

V. Conclusion

In this paper, an alternative hybrid approach was proposed based on a few practical KPIs collected from field measurements, derived from the definition of the 3GPP theoretical equation for calculating the maximum throughput. This approach provides theoretical predictions with hourly granularity. Several tests were conducted in different real usage scenarios: one group focusing on regular traffic on ordinary days, and another group addressing traffic on atypical days, such as live music concerts. Differences between the asymmetric downlink and uplink traffic were also observed.

From the analysis of regular traffic, an important behavior was observed: a clear correlation between hybrid theoretical throughput predictions and measured throughput. Convergence is achieved by using a multiplicative scale factor (SF) to the theoretical predictions. It was observed that a single SF value was valid for an entire day's dataset. The SF values were higher for downlinks compared to the values observed for uplinks. This is primarily due to the actual use of the allocated PRBs during the whole time they are made available. In uplinks, the PRBs are usually more intensively occupied, leading to low SF values.

The analysis of the atypical days' scenarios somehow corroborated that hypothesis. As traffic dramatically increased throughout such atypical days, a single SF value could not maintain the convergence between predictions and measurements. The larger the traffic, the more the allocated PRBs were fully occupied, lowering the SF needed to achieve the expected convergence. The uplink dataset analysis also presented results consistent with this rationale.

Therefore, this work indicates an interesting path for using the 3GPP model for capacity analysis, combined with KPIs from real data, to propose simple semi-empirical capacity prediction models. These models can serve as support for 5G network planning or realistic simulation-based studies. However, further studies are recommended to fully map other system factors that could better explain the need for the scale factor and how it could be predicted automatically from other practical KPIs or system parameters, leading to a more robust prediction model.

References

[1] 3GPP TS 38.306, "NR; User Equipment (UE) radio access capabilities," v15.7.0 Release 15, Valbonne, France, 2019. [Online]. Available: https://portal.3gpp.org/desktopmodules/Specifications/SpecificationDetails.aspx?specificationId=3193.

[2] 3GPP TS 36.213, "Evolved Universal Terrestrial Radio Access (E-UTRA); Physical layer procedures," v14.2.0 Release 14, Valbonne, France, 2017. [Online]. Available: https://portal.3gpp.org/desktopmodules/Specifications/SpecificationDetails.aspx?specificationId=2427.

[3] H. Kim, "Coding and modulation techniques for high spectral efficiency transmission in 5G and satcom," in: *23rd European Signal Processing Conference*, pp. 2746–2750, August 31 – September 4, Nice, France, 2015, doi: 10.1109/EUSIPCO.2015.7362884.

[4] 3GPP TR 38.802, "Study on New Radio Access Technology; Physical Layer Aspects," v14.2.0 Release 14, Valbonne, France, 2017. [Online]. Available: https://portal.3gpp.org/desktopmodules/Specifications/SpecificationDetails.aspx?specificationId=3066.

[5] A. de Javel, "5G RAN: physical layer implementation and network slicing. Networking and Internet Architecture," Doctoral Thesis, Institut Polytechnique de Paris, Paris, France, 2022. [Online]. Available: https://theses.hal.science/tel-03848017.

[6] J.Vihriälä, A. Zaidi, V. Venkatasubramanian, N. He, E. Tiirola, J. Medbo, E. Lähetkangas, K. Werner, K. Pajukoski, A. Cedergren, R. Baldemair, "Numerology and Frame Structure for 5G Radio Access," in: *IEEE PIMRC2016*, pp. 1–5, September 4-8, Valencia, Spain, 2016, doi: 10.1109/PIMRC.2016.7794610.

[7] E. Dahlman, S. Parkvall and J. Skold, *4G, LTE-Advanced Pro and the Road to 5G*, 3rd ed. Academic Press, 2016.

[8] J. Martinez, J. Moreno, D. Rivera and J. Berrocal, "Radio Access Evaluation of Commercial 5G Service," *Electronics*, vol. 10, no. 22, article id 2746, pp. 1–11, November 2021, doi: 10.3390/electronics10222746.

[9] R. Saha, J. Cioffi, "Dynamic Spectrum Sharing for 5G NR and 4G LTE Coexistence – A Comprehensive Review," *IEEE Open Journal of the Communications Society*, vol. 5, pp. 795–835, January 2024, doi: 10.1109/OJCOMS.2024.3351528.

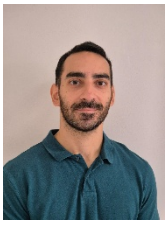

Rômulo Torres Serra holds a degree in Telecommunications Engineering from the Celso Suckow da Fonseca Federal Center for Technological Education (CEFET/RJ), earned in 2017, and a master's degree in Electrical Engineering from CEFET/RJ, completed in 2024. He has been a network planning engineer at TIM BRASIL since 2018. His work and interests focus on the field of Telecommunications Systems.

Maurício Henrique Costa Dias holds a degree in Communications Engineering from the Military Institute of Engineering (IME), earned in 1992; a master's degree in Electrical Engineering from IME, completed in 1998; and a doctorate in Electrical Engineering from the Pontifical Catholic University of Rio de Janeiro (PUC-Rio), concluded in 2003. He performed postdoctoral research on reconfigurable antennas at the Grenoble Institute of Technology in 2013. He worked at IME as a professor and researcher from 2003 to 2012 and again from 2015 to 2017. Since 2018, he has been a professor at CEFET/RJ. His main area of expertise is Applied Electromagnetism, with an emphasis on Antennas, Propagation, and Electromagnetic Compatibility.